Toughness and Ductility of Heavy-Walled Ferritic Spheroidal-Graphite Iron Castings

Yoshitaka IWABUCHI*, Hideki NARITA** and Osamu TSUMURA**

Abstract

Spheroidal-graphite(s-g) iron castings recently have exceeded 160 metric tons in shipping weight, since there has been an increasing application of s-g iron to heavy castings. Increasing the size of s-g iron castings results in difficulty in obtaining high ductility and toughness. This paper described the fundamental study concerning with elongation and fracture toughness and discussed the material data obtained from mock-up casks with 500 mm in wall thickness made of s-g iron.

Key words : Fracture Toughness, Spheroidal Graphite Iron, Ferrite Matrix, Nodularity, Elongation

1.Introduction

Spheroidal graphite (s-g) cast irons having ferritic matrix, possess improved ductility together with good castability, and therefore they have increased application to not only machine parts, but also to such heavy castings as mill stands and spent fuel casks which require high quality and reliability.[1]-[6]

It is well known that increasing weight and wall-thickness of the iron castings degrade the several properties.[2],[3] The graphite morphology in the thermal center of s-g iron castings with heavy wall-thickness is often degenerated by magnesium fading and chemistry segregation, which seriously impairs several mechanical properties especially elongation. Therefore, there is a difference in mechanical properties between the test coupons separately cast and the specimens taken from the heavy castings, which results in difficulty of obtaining a reliability of s-g iron castings. Although the degradation of the mechanical properties is presumed to be related to the microstructural change through the wall-thickness, there has been little systematic work in heavy castings.

In this work, elongation, impact energy and fracture toughness are shown to correlate with graphite morphology. Prior work[1]-[14] on fracture toughness in s-g iron castings is reviewed and selectively applied to the present work in order to clarify fracture toughness and its relation to microstructural features. The results of systematic examination in mock-up casks[15]-[22] made of ferritic s-g iron are intended to lead to the concluding remarks of this work.

2.Experimental

The heats were melted in a 10 ton basic electric furnace and poured into three sand molds with 480 mm wall thickness which were cooled in various ways to obtain the different morphology of the graphite nodule. The Mg treatment and inoculation were performed by using the commercially obtainable agents. Optimum chemistry was selected so as to obtain the ferritic matrix, and each heat has the almost same chemical composition as the commercial level as shown in Table 1.

Table 1 Chemical composition of each casting used for this study

Casting	C	Si	Mn	P	S	Mg	Remarks
A	3.62	1.74	0.22	0.019	0.004	0.050	indirect chill
B	3.63	1.75	0.19	0.025	0.003	0.055	direct chill
C	3.64	1.65	0.19	0.023	0.004	0.053	mist cooling

*Department of Mechanical Engineering, Kushiro National College of Technology,
**Muroran Plant, Japan Steel Works Co. Ltd.

These castings were subjected to annealing at 1173K as ferritizing. Graphite nodularity of several specimens was measured in accordance with the standard of Japan Foundrymen's Society. Fractions of ferrite and graphite were measured by a point-counting method. The average nodule diameter was calculated, assuming they have a spherical geometry and neglecting the small nodule below 10μ m in diameter.

Charpy impact tests using 2 mm V notch specimens were carried out at an ambient temperature as well as tensile tests using round bar specimens of 14 mm diameter and 50 mm gauge length. Elastic-plastic fracture toughness J_{IC} was measured by a compliance method in accordance with ASTM E813-81 using 1T-CT specimens with side groove.

3 Results and discussion

3 1 Factors affecting ductility

Improved ductility is characteristic of s-g iron castings with ferritic matrix, however, increasing wall-thickness is expected to results in its degradation due to the strong mass effect of s-g iron castings. Satisfactory regression analysis[1] describing the relation of elongation to the microstructural features of s-g iron castings has been presented as equation (1).

$$Elongation(\%) = -20 - 0.59(Si)^2 - 26(Mn)^2 - 52P + 0.32n - 0.031N_g + 0.015(\quad -25)^2 \quad \ldots\ldots(1)$$

Where Si, Mn and P are concentration of each element in mass percent, n is graphite nodularity(%), N_g is nodule count(mm^{-2}) and   is pearlite fraction(%).

Hereafter, the factors affecting elongation of s-g iron castings are discussed.

3 1 1 Effect of pearlite fraction

It is well known that increasing pearlite fraction increases tensile strength and decreases elongation in various steels[23],[24]. Therefore s-g iron castings should be subjected to ferritization to improve the ductility. Ferritization of the iron is divided into direct transformation in which unstable austenite decomposes to graphite and ferrite, and indirect transformation in which unstable austenite firstly transformed pearlite and subsequently it decomposes to graphite and ferrite[25],[26]. Figure 1 shows the ferritization curves which indicate the relation between ferrite fraction and the isothermal annealing. Indirect ferritization fastly proceeds at the temperature(993K) just below A_{C1}. Comparing the effect of nodule size on the ferritization, small graphite nodule is preferable to large one.

Figure 2 shows the effect of pearlite fraction on elongation as a function of nodularity in s-g iron castings.[6] Elongation decreases with increasing pearlite fraction, since the plastic deformation of matrix is restricted by pearlite[27]. However pearlite fraction has little effect on elongation, when nodularity is so low that the graphite acts as notch leading to low ductility.
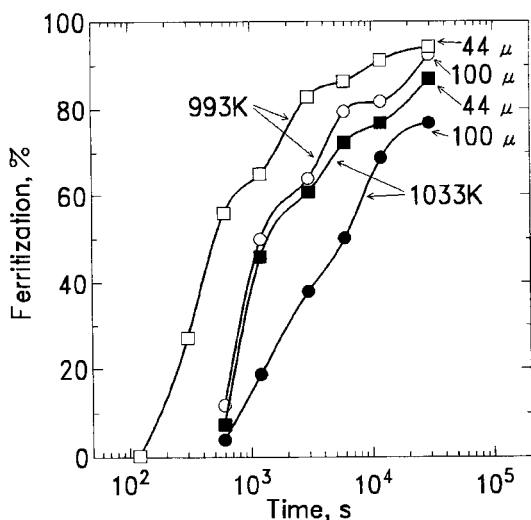

Fig.1 Variation of ferritization between two specimens having large and small graphite nodulels with isothermal heating
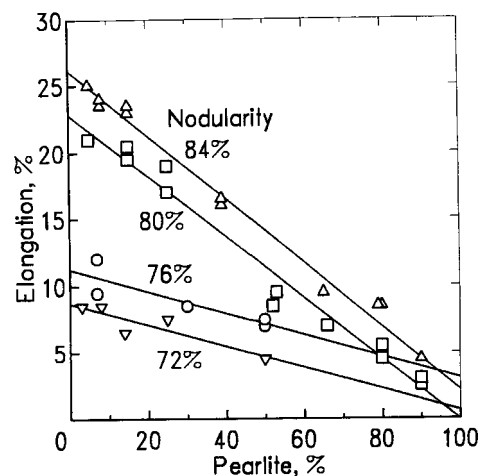

Fig.2 Relation between elongation and pearlite fraction of graphite nodularity

3 1 2 Effect of graphite nodularity

Although graphite nodularity is a important factor affecting elongation as shown in Fig. 2, it is degenerated by fading of magnesium, segregation of nodularity-impairing elements and low-melting elements, and coaurlecense of graphite, when the wall-thickness of the castings is increased. Figure 3 shows the effect of nodularity on elongation in s-g iron castings with more than 90% ferritization as a function of nodule size. Elongation is relatively low below 75% nodularity and it proportionally increases with nodularity when it exceeds 75%.

Tensile fracture of s-g iron castings is performed in the way that each void creates in the graphite nodule and at the boundary between the matrix and the graphite nodule, and subsequently links each other. When the graphite nodularity deteriorates, it can be assumed that notch effect of graphite is emphasized and consequently increases the stress concentration factor. Degradation of nodularity decreases elongation due to notch effect of graphite nodule, which leads the fast propagation of the crack at the boundary between the graphite and the matrix.

It has been presented in literatures[23] that the stress concentration factor of s-g iron castings ranges from 1.6 to 3.0. Nominal stress concentration factor α_k due to graphite nodule is expressed as equation (2) by using tensile strength of cast iron σ_c and steel σ_s respectively, both of which both have same hardness, effective area[28] A_{ef} and graphite nodule fraction N_A.

$$\alpha_k = A_{ef} \cdot \sigma_s / \sigma_c = (1-N_A) \sigma_s / \sigma_c \quad \cdots\cdots \quad (2)$$

Although α_k increases with the decrease of nodularity, α_k of s-g iron castings with nodularity exceeding 75% falls within the range from 0.92 to 1.11.[11] The evidence that α_k is roughly equal to 1 and below 1 means that the plastic deformation of the ferrite around the graphite nodule results in the decrease of the stress concentration factor macroscopically.

Degradation of nodularity is presumed to be resulted from the delayed solidification time due to increasing wall-thickness of castings. Figure 4 shows the effect of solidification time on nodularity and nodule size in s-g iron castings. It is clear that there is good relation between solidification time and nodularity indicating that nodularity of more than 75% can be obtained when the castings solidify within 2.5h.
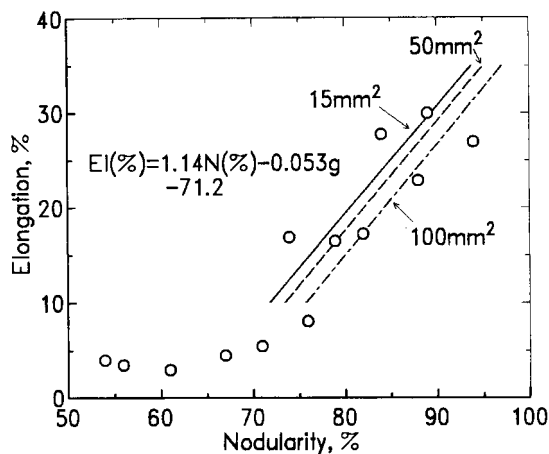

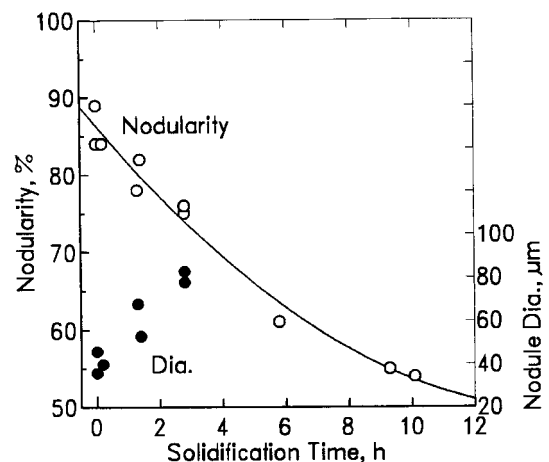Fig.3 Relation between elongation and graphite nodularity of the specimens with more than 75 %ferrite fraction

Fig. 4 Relation between graphite nodularity and solidification time

3 1 3 Effect of graphite nodule count

Tensile fracture of ferritic s-g iron castings is performed by creating the voids due to the graphite nodule and linking between them. Therefore elongation increases with decreasing nodule count, since effective area A_{ef} through which the crack propagates increases and consequently the plastic deformation of ferrite matrix increases when nodule count decreases.

Volume fraction of graphite nodule V_g is expressed as $V_g=0.032(\%C)$ by using graphite density($2.33g/cm^3$) and ferrite density($7.70g/cm^3$). Area fraction of graphite nodule N_a, which agrees with V_g, is related to nodule size, i.e. nodule

diameter D and nodule count N_g by equation (3).

$$N_a = \pi D^2 N_g/4 \quad \ldots\ldots(3)$$

Therefore elongation depends on nodule diameter, and it is related to nodule count where each casting has almost the same content of carbon.

Figure 5 shows the effect of nodule size on elongation of ferritic s-g iron castings. Elongation increases with increasing nodule diameter and reaches the maximum. Thereafter elongation decreases when nodule diameter exceeds about 75 μm, which is supposed to be due to the notch effect of the local roughness of each graphite nodule resulted from the absorption of the small nodules on the dominant large nodules.

3 1 4 Effect of alloy chemistry

Recommended concentration of carbon and silicon to obtain s-g iron castings without primary cementite are determined by both maximum and minimum wall-thickness of the castings concerned. Manganese deteriorates nodularity since it easily segregates during solidification. Increasing the size of s-g iron castings causes the formation of chunky-graphite and inter-cell flake-graphite. Chunky-graphite-forming elements are Ni, Si, Ca and Ce, and inter-cell-graphite-forming elements are Cu, Sn, Al, As and Sb in order of its tendency respectively. These elements of each group do diametrically harm to graphite morphology and their detrimental effect is cancelled by each other.

Fig. 5 Relation between elongation and graphite nodule diameter as a function of nodularity

Addition of small amounts of rare-earth metal and antimony is effective to suppress chunky- graphite, and its effect has been discussed elsewhere[29],[30].

3 2 Relation between fracture toughness and microstructure
3 2 1 Evaluation of elastic-plastic fracture toughness

Fracture toughness of s-g iron castings with ferrite matrix should be evaluated by elastic-plastic fracture mechanics using J_{IC} and COD(δ) because of high ductility. The purpose of this section is to give an overview of the relationship between elastic-plastic fracture toughness and microstructural features[7]-[12].

Elastic-plastic fracture toughness J_{IC} has been determined by R-curve method(RC) which detected the start of ductile tearing. In s-g iron castings with a ferrite matrix, J_{IC} was evaluated by means of electric potential(EP), acoustic emission(AE), compliance(CM) and ultrasonic(US) single specimen methods, giving equation (4)[8],[12].

$$J_{IC}(RC) = J_{IC}(CM) = J_{IC}(US) = 1.34\{J_{IC}(AE), J_{IC}(EP)\} \quad \ldots\ldots(4)$$

J_{IC} is generally related to crack opening displacement δ as $J_{IC} = m\sigma_f\delta$ using flow stress σ_f(average of yield stress σ_y and ultimate stress σ_B) and constant m(m=1～3) depending on matrix. Ductile tearing of J_{IC} test specimen is performed in the way that each void creates in the graphite nodule and at the boundary between the matrix and the graphite nodule, and subsequently links each other. Therefore, J_{IC} is expressed as $m\sigma_f X$ supposing that criterion of fracture is determined by $m\sigma_f$ where δ accords inter-void distance X. Finally J_{IC} is expressed as equation (5)[8] since X is expressed as a function of nodularity n and nodule size D.

$$\begin{aligned} J_{IC} &= m\sigma_f\delta \\ &= m\sigma_f X \\ &= m\sigma_f\{X_0 - 1/2(Dn^{-1/2} - Dn^{3/2})\} \\ &= m\sigma_f\{N_g^{-1/2} - 1/2(Dn^{-1/2} - Dn^{3/2})\} \quad \ldots\ldots(5) \end{aligned}$$

J_{IC} is converted into fracture toughness K_{IC} by $K_{IC}(J) = \{J_{IC}E/(1-\nu^2)\}^{1/2}$, where Young's modulus E is 171,000MPa corresponding to average value of each specimen and Poisson ratio ν is 1/3. Figure 6 shows the plotting of fracture toughness[10],[11] of s-g iron castings against nodule size. Uncertainty exists in the relation between nodule size and fracture
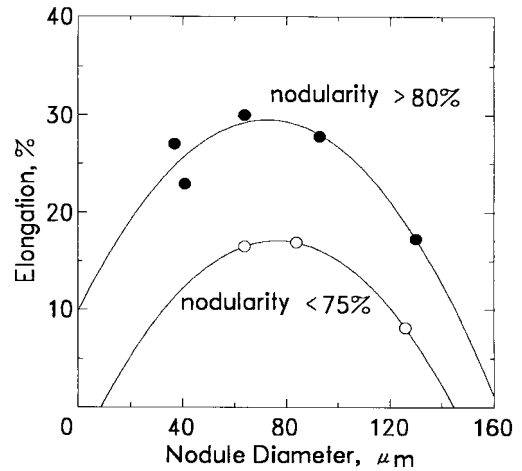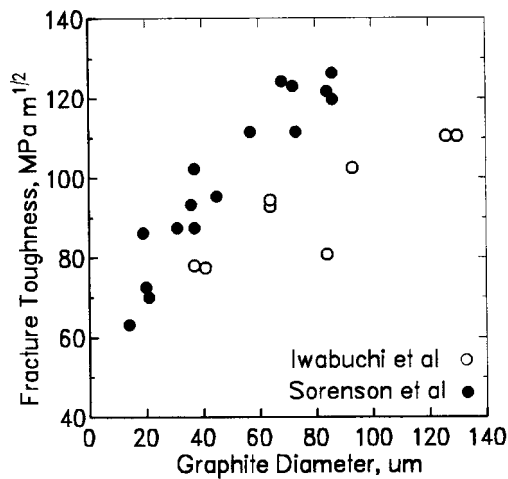
Fig.6 Relation between fracture toughness and graphite nodule diameter of ferritic ductile cast iron
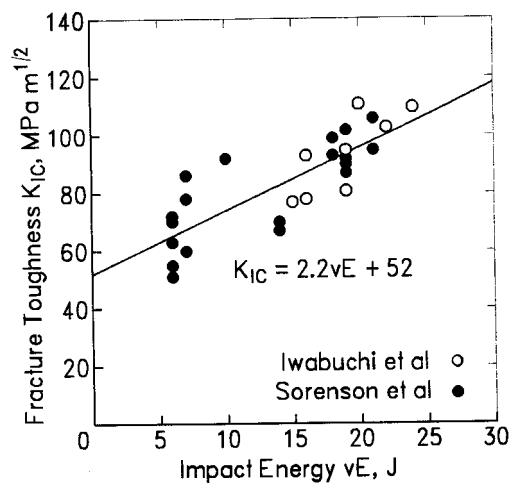

Fig.7 Relation between fracture toughness and Charpy 2mm -V notched impact energy of ferritic ductile cast iron

toughness showing relatively wide dispersion between them, however, it is supposed that fracture toughness at ambient temperature tends to be improved with increasing nodule size.

Although the quantity measured in the impact test is not directly useful in a design of the structures, Charpy V-notch impact test has retained high degree of utility and use, since it is simple and quick to make the results. Fracture toughness was correlated[31]-[33] with tensile strength, yield strength and impact energy. Regression equation[32] was developed which satisfactorily predicted fracture toughness, and equation (6) was presented in the upper shelf range of steels.

$$(K_{IC}/\sigma_y)^2 = 0.6464[(\sigma_{2v}E_{upp}/\sigma_y) - 0.0098] \quad \ldots\ldots\ldots\ldots(6)$$

Figure 7 shows the plotting of fracture toughness against impact energy at ambient temperature.[10],[11] Although there is some scatter, a trend appears between them.

Below the transition temperature, the eutectic cell boundary and matrix are important factors affecting fracture toughness and the graphite nodules play the role of a crack-arresting element, since the brittle fracture predominantly occurs in this region. For the behavior of J_{IC} in regard to microstructural parameter, it is reasonably deduced that the dominant factor is nodule size over the ductile fracture region and nodule count in the transition region[9],[12].

3 2 2 Evaluation of dynamic fracture toughness

Fracture toughness depends on the loading speed. Dynamic elastic-plastic fracture toughness J_{Id} is evaluated[11],[13] by using CT-specimens in which hydraulic servo testing instruments and drop-weight type tension testing instruments are employed. The start of ductile tearing is detected by the same methods as those of J_{IC}. Instrumented Charpy impact testing method[14] has been proposed to evaluate dynamic fracture toughness. Constant J_{Id} value was obtained by using the side grooved Charpy type specimen with the thickness of 20 mm.

Figure 8 shows stress intensity rate K dependence on fracture toughness at 233K and 50% ductile-brittle fracture transition temperature T of s-g iron castings with ferritic matrix.[13],[14],[34]. Fracture toughness decreases when K exceeds 10^2 MPa m$^{1/2}$ s^{-1}, and above about 10^3 MPa m$^{1/2}$ s^{-1} it reaches constant value. T is shifted to a high temperature side with increasing K. The linear[13] relation between 50% ductile-brittle fracture transition temperature T_{rs} and logarithm stress intensity rate K is expressed as equation (7).

$$T_{rs}(K) = 12.7 \log K(MPa \ m^{1/2} \ s^{-1}) + 195 \ldots\ldots\ldots(7)$$

Unlike J_{IC} the distribution of graphite nodule has a very slight effect on J_{Id}[13]. J_{Id} in the upper shelf region increases with increasing K, which is mainly attributed to increase in strength at high rate of K[13]. Therefore J_{Id}/σ_y in the shelf region can be used as a material constant irrespective of stress intensity rate K and temperature.

3 3 Quality of ferritic ductile iron cask

3 3 1 Safety evaluation and quality assurance of casks

It is an important thing for use in spent fuel cask that there is no brittle failure against any expecting severe damage and a quality assurance method must be established to evaluate the potential for brittle failure[15]-[17]. Table 2 shows the draft specification requirement[22] of tensile and impact tests. At present there is no specification that define minimum material properties acceptable for this intended application, however, it is required that the spent fuel cask is able to withstand the 9-meter horizontal drop and there is no crack initiation from the artificial fraw on the body surface. Due to the potential for brittle failure a discipline of importance is fracture toughness. The stress intensity rate ranging from 10^2 to 10^3 MPa m$^{1/2}$ s^{-1} corresponds to that which likely to be expected for spent fuel casks subjected to the 9-meter horizontal drop. From Fig. 8, it is clear that fracture toughness of s-g iron castings falls within constant value in this stress intensity rate range irrespective of K.

As for quality assurance of cast iron casks, large test specimens actually can not be taken from the product castings. Therefore the technology of non-destructive examination and certification test using small specimens are desirable. It has been established that there is some consistent relationship between fracture toughness and interrelated microstructural parameters such as graphite nodule size, nodule count or nodularity coupled with charpy impact energy[8]-[14].

Table 2 Mechanical properties requirement of the cast iron cask

Yield Strength (MPa)	Tensile Strength (MPa)	Elong. (%)	Impact Energy (J)
≧200	≧300	≧8	≧4

In addition to microstructural features affecting elongation, elongation could be related to other mechanical properties. Figure 9 shows the linear relation of elongation to tensile strength of s-g iron castings with ferritic matrix. Impact energy and fracture toughness were previously shown to be linearly related in Fig. 7. The lower limit of the relation[16] between impact energy $_{2v}E_{-40}$ and fracture toughness K_{IC} at 233 K is expressed as equation (8) depending on yield strength $_y$.

$$K_{IC}(MPa\ m^{1/2}) = 403(_vE_{-40}/_y)^{1/2} \quad \ldots\ldots(8)$$

Maximum transmission ultrasonic frequency increases with improving graphite morphology which affects fracture toughness[16], so that, ultrasonic examination is presumed to ensure the material properties then guarantee the internal quality of spent fuel casks made of s-g iron.
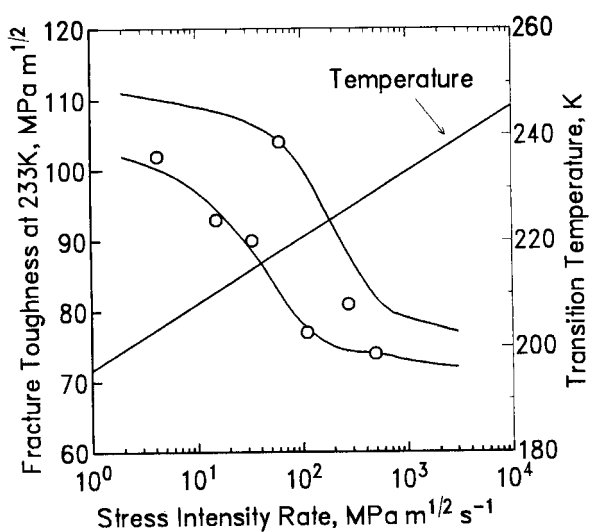

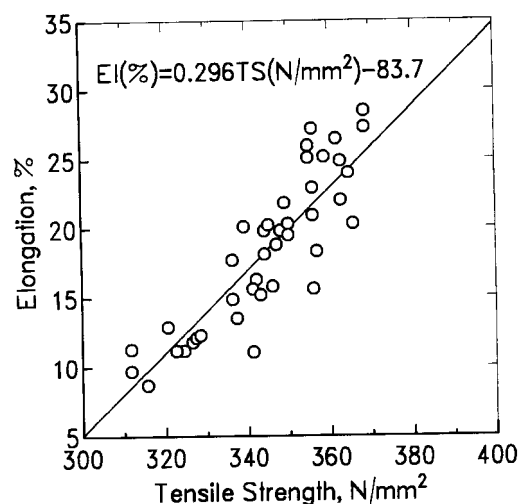Fig.8 Stress intensity rate dependence on fracture toughness at 233 K and transition temperature

Fig.9 Relation between elongation and tensile strength of ferritic ductile cast iron

3 3 2 Mechanical properties and fracture toughness of mock-up casks

The cast iron casks have cylindrical configuration with a bottom end and 350-500 mm heavy wall-thickness exceeding 100 metric tons in shipping weight. Mock-up casks, which have 2.0-2.5 m in outer diameter and 1.8-2.5 m in height, were manufactured and a systematic examination[18]-[22] was carried out to study its practical utilization of s-g cast iron.

Ferrite fraction in mock-up casks which are as-cast or ferritized is more than 94 % and its density falls within the range of 6.98 to 7.12 g/cm^3 at all locations. Graphite nodularity which affects mechanical properties and fracture toughness spans from 65 to 96 % according to each casting or its location.

Tensile test was performed at the temperatures between 233 and 673K using the specimens taken from each location of mock-up casks. Figure 10 shows the resulting data from tensile test illustrating their average and minimum properties. Although some scatter exist at each location of mock-up casks, elongation corresponds to graphite nodularity and exhibits 12 % on the average.

Charpy 2 mm V-notched impact test was performed at the temperatures between 233 and 473K. Figure 11 shows the resulting data from impact test illustrating transition temperature and impact energy at 233K together with shelf energy. All mock-up casks exhibits higher energy than aiming value and lower transition temperature than 300 K.

Fracture toughness was measured by instrumented Charpy method and conventional CT method using 1T, 3T and 6T-CT specimens taken from the weakest location of mock-up casks. Figure 12 shows the fracture toughness at each testing temperature, where the elastic-plastic fracture toughness is converted into K_{IC}. It can be seen that this method gives dynamic fracture toughness values near the lower boundary values as obtained by conventional CT methods.

Figure 13 shows the graphical representation of Weibull's plot[16],[21] of fracture toughness measured by 9T-CT specimens taken from several mock-up casks, thus substantiating the good fitting by equation (9).

$$P(K_{IC}) = 1 - \exp\{-(K_{IC}/76.2)^{11}\} \quad \ldots\ldots\ldots(9)$$

Stress intensity factor on the position which the 9-meter horizontal drop inflicts the maximum damage is supposed to be 20.9 MPa m$^{1/2}$. Therefore there could not be the possibility of loss of s-g cast iron cask integrity after a impact load, since the probability of its falling below this value is a 6.4×10^{-7} from equation (9).
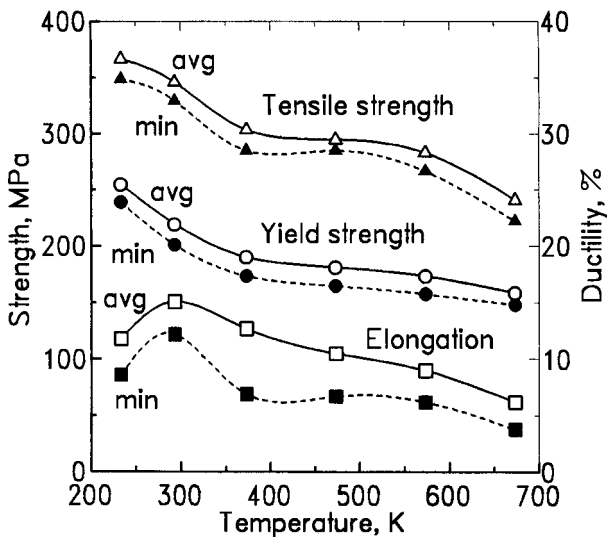

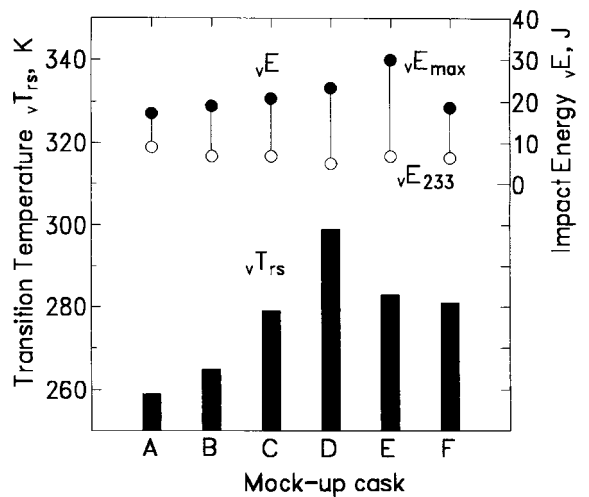Fig.11 2 mm V-notched impact properties of the from each location of 6 mock-up casks with testing temperature

Fig.10 Variation of tensile properties of the specimens taken specimens taken from each location of 6 mock-up casks
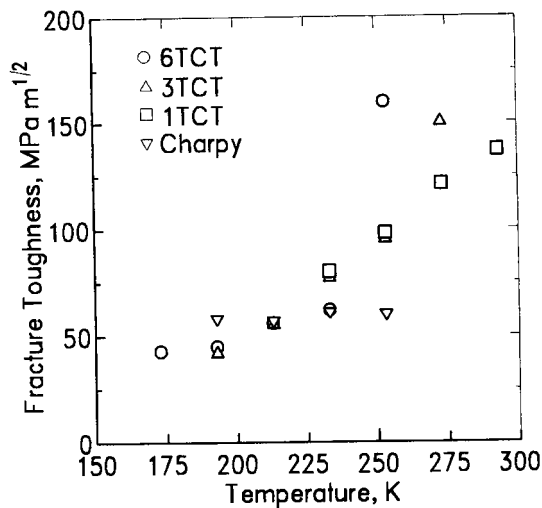
Fig.12 Fracture toughness measured by instrumented
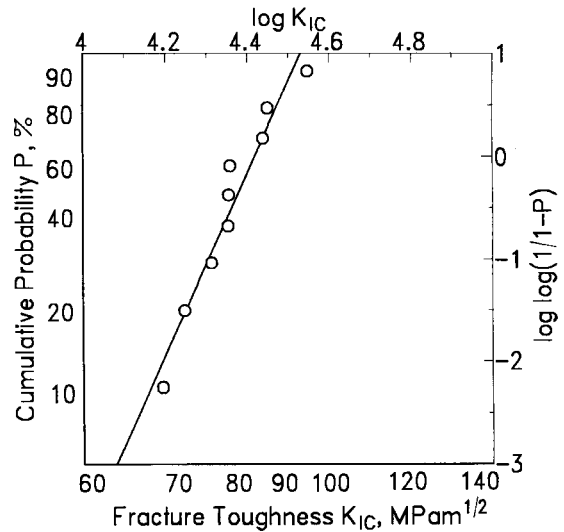Charpy and Ct methods for a mock-up cask

Fig.13 Weibull's plot of fracture toughness measured
by 6T-Ct method at 233 K for mock-up casks

4. Conclusions

S-g iron castings with ferritic matrix exhibit improved toughness and ductility and their systematic fundamental studies lead the establishment of a manufacturing processes for heavy-walled castings. Aiming at ferritic s-g iron for real use in spent fuel casks, microstructural analyses were performed on heavy-walled castings to ensure the accurate correlation between microstructure and material property, and subsequently its certification test was performed positively to propose the idea of criteria and quality assurance.

Based upon the data regarding the fracture toughness and quality assurance together with its relatively low cost, the potential use of s-g iron castings would be expected for diverse machine parts with high quality and reliability.

References

(1) T.Okada and Y.Maebashi : Imono, (1971), 43, p.291-292

(2) Morozumi and M.Ishihara : Imono, (1976), 48, p.532-541

(3) T.Okada and Y.Maebashi : Imono, 1971, 43, p.649-658

(4) T.Kobayashi : (1985), 3, p.7-15

(5) H.Yamamoto, T.Meguro and I.Kimura : the 16th JFS symposium, Tokyo, (1985) , p.32-39

(6) Y.Iwabuchi, H.Narita and Y.Ichinomiya : Imono, (1987), 59, p.153-158

(7) T.Kobayashi : Bull.JIM, (1979), 18, p.512-517

(8) K.Kuribayashi, T.Kishi, P.Phandhubanyong, M.Ito, T.Umeda and Y.Kimura : Tetsu-to-Hagane, (1983), 69, p.663-670

(9) T.Kobayashi and H.Yamamoto : (1987), 59, p.573-579

(10) P.McConnell, P.Lombrozo, J.Santucci and K.Sorenson : the 91st AFS Casting Congress, St.Louis, (1987) , p.147-201

(11) Y.Iwabuchi, H.Narita and O.Tsumura : Imono, (1988) ,60, p.215-220

(12) K.Nakano and K.Yasunaka : Tetsu-to-Hagane, (1992), 78, p.926-933

(13) K.Nakano and K.Yasunaka : Tetsu-to-Hagane, (1994), 80, p.330-335

(14) T.Kabayashi, H.Yamamoto and K.Matsuo : Imono, (1988) , 60,p.110-115

(15) Central Research Institute of EPI, (EPRI Technical Report L87002, (1987)

(16) Y.Harada, N.Urabe and M.Imai : Fuel, J.Nuclear Power Industry, (1988), 34, p.53-57

(17) Y.Tanaka, H.Koeda and K.Kayano : Trans. Japan. Soc. Mech. Eng.   ,940-30, (1994) , p.520-523

(18) S.Nakamura, N.Sakamoto, K.Inoue, K.Ohgi and K.Matsuda : Imono, (1987), 59, p.664-669

（19）T.Yanaka, H.Saitou, D.Sakurai and H.Arata : Imono, （1988）, 60, p.20-25

（20）Y.Iwabuchi, H.Narita, M.Murata, S.Simizu and O.Tsumura : Imono, （1988）, 60, p.167-172

（21）R.Kusakawa : Text of course, JFS, （1988）, p.50-58

（22）D.Sakurai and M.Minami : Imono, （1992）, 64, p.114-119

（23）K.Ikawa and Y.Tanaka : Casting and Forging, （1977）, 8, p.3-10

（24）S.Komatsu, T.Shiota and K.Nakamura : Imon, （1988）, 60, p.643-648

（25）T.Ohwadano, M.Nishimura and H.Moyata : Imono,（1972）, 44, p.666-673

（26）Y.Iwabuchi and I.Kobayashi : Research Reports Kushiro National College of Technology, （1992）, 28, p.33-39

（27）A.Harada, M.Yano, T.Endou and N.Kawaguchi : Prepr. of JSM, （1987）, No.87-0789, p.1-8

（28）T.Shiota and S.Komatsu : Imono, （1977）, 49, p.602-607

（29）O.Tsumura, Y.Ichinomiya, T.Miyamoto and T.Takenouchi : Imono, （1995）, 67, p.540-545

（30）O.Tsumura, Y.Ichinomiya, T.Miyamoto and T.Takenouchi : Imono, （1996）, 68, p.54-60

（31）T.Iwadate, Y.Tanaka, H.Takenaka and S.Tarashima : Zairyou, （1986）, 35, p.873-879

（32）H.Mimura : Testu-to-Hagane, （1978）, 64, p.906-916

（32）S.Nunomura and M.Nakashiro : Testu-to-Hagane, （1978）, 64, p.860-869

（34）N.Urabe, T.Nishimura and K.Yamanaka : Prep. of JFS., Akita, (1986), p.25